Photofissility of ^{232}Th measured with tagged photons from 250 to 1200 MeV

N. Bianchi, A. Deppman,* E. De Sanctis, A. Fantoni, P. Levi Sandri, V. Lucherini, V. Muccifora, E. Polli, A. R. Reolon, P. Rossi, A. S. Iljinov,† M. V. Mebel,† and J. D. T. Arruda-Neto‡
Istituto Nazionale di Fisica Nucleare, Laboratori Nazionali di Frascati, P.O. Box 13, I-00044 Frascati, Italy

M. Anghinolfi, P. Corvisiero, G. Gervino,§ L. Mazzaschi, V. Mokeev, G. Ricco, M. Ripani, M. Sanzone, M. Taiuti, and A. Zucchiatti
Istituto Nazionale di Fiscia Nucleare and Dipartimento di Fisica dell'Universitá di Genova, I-16146, Genova, Italy

R. Bergère, P. Carlos, P. Garganne, and A. Leprêtre
DAPNIA/SPhN, CEN, Saclay, Gif-sur-Yvette Cedex 91191, France
(Received 9 April 1993)

The photofission cross section of ^{232}Th was measured in the energy range 250–1200 MeV using a monochromatic tagged photon beam and a parallel-plate avalanche detector. The ^{232}Th nuclear photofissility was obtained by measuring simultaneously and in the same energy range the photofission cross section of ^{238}U and assuming a photofissility equal to one for ^{238}U. It was found that, contrary to the case for heavier actinides, the ^{232}Th photofissility value does not saturate up to 1200 MeV. Rather, it lies between 0.6 and 0.8, and shows a weak energy dependence: it increases by about 15% over an interval of 1 GeV. A comparison of these experimental findings with the predictions of an intranuclear-cascade Monte Carlo calculation is given.

PACS number(s): 25.20.Lj, 25.85.Jg

I. INTRODUCTION

The photofission reaction is a powerful tool for investigating the complex dynamics of the excitation of heavy nuclei, due to the well-known properties of the electromagnetic interaction and to the large cross section for this process.

The photofission of heavy nuclei is well described by the concept of a two-step process [1]: (i) In the fast first step, the projectile initiates a cascade of subsequent independent collisions of the primary and secondary fast particles with the intranuclear nucleons. This intranuclear cascade leads to the formation of a highly excited thermalized compound nucleus, which is characterized by A_{CN} nucleons, Z_{CN} protons, an angular momentum l, and an excitation energy E^*. (ii) In the slow second step, the excited nucleus evaporates particles successively or undergoes fission, depending strongly on the variables Z^2_{CN}/A_{CN} and E^*.

Photofission experiments have been performed since the earliest days of photonuclear studies [2]. Nevertheless, in spite of the considerable effort spent so far on the field, the knowledge of the photofissility, W_f, of heavy nuclei is still unsatisfactory. The W_f of a nucleus of given Z and A is generally defined as the probability that this nucleus undergoes fission, and is measured experimentally as the ratio of the photofission cross section $\sigma_f(k)$ and the total inelastic cross section $\sigma_T(k)$, where k is the photon energy.

The lack of reliable data is particularly evident in the energy region above the pion threshold, where the observed disagreement among the data probably can be ascribed to the unfolding methods used to extract the cross sections from the yields of bremsstrahlung photons on thin target foils, and to the poor discrimination of fission events from the background of other inelastic reaction products. Good reviews of these "old technique" experiments, performed mainly during the 1960s and the 1970s can be found in Refs. [3] and [4]. Recently the development of new techniques for producing monochromatic tagged photon beams and the availability of parallel-plate avalanche detectors (PPADs) have brought the photofission reaction into the forefront of experimental and theoretical interest.

As an example, in Fig. 1 are shown the photofission cross section values, normalized to the mass number A, for ^{238}U, obtained in the most recent experiments performed using tagged photons and PPADs [5–7]. As shown the data agree among themselves within the total experimental errors; notice that the errors shown in Fig. 1 are statistical only, and systematic errors between 5% and 10% should be added to them. Also shown in the figure are the upper and lower limits of the "universal behavior" of the total cross section per nucleon, obtained in the Δ region from measurements on several nuclei carried out with various techniques (for a review see Ref.

*Present address: Physics Institute, University of São Paulo, São Paulo, Brazil.
†Permanent address: Institute for Nuclear Research of the Academy of Sciences of Russia, Moscow 117312, Russia.
‡Permanent address: Physics Institute, University of São Paulo, São Paulo, Brazil.
§Permanent address: Dipartimento di Fisica dell'Universitá di Torino, I-10125, Torino, Italy.

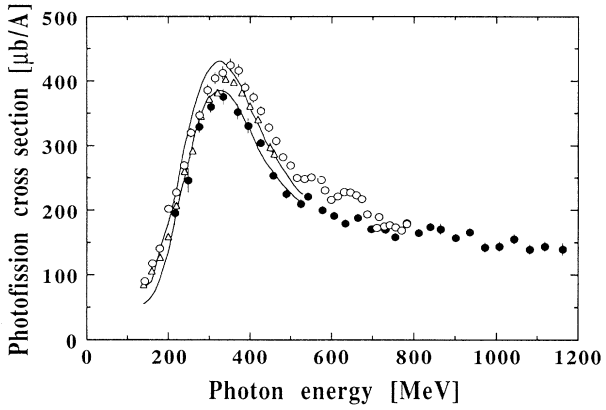

FIG. 1. ^{238}U photofission cross section data normalized to the mass number A, measured with tagged photons above the pion threshold: Ref. [5] (closed circles), Ref. [6] (open circles), Ref. [7] (open triangles). The area between the two curves represents the universal behavior of the total nuclear cross section (see the review in Ref. [8]).

[8]). As can be seen, the fission cross section data for U saturate the total cross section, so that uranium fissility is generally assumed equal to 1. Also, the monochromatic-photon data at lower energies [9,10] confirm that the photofissility for heavy actinides has an almost constant value very close to unity for energies above a few tens of MeV. For these very heavy nuclei, having values of $Z^2/A > 35$, the fission barrier B_f is very low (5–6 MeV) and shows a double-humped structure due to strong oscillations of the shell correction with deformation.

Very different is the behavior of preactinide nuclei ($Z^2/A < 35$), such as ^{197}Au and ^{209}Bi, for which experimental data [11,12] show a strong energy dependence of photofissility above the pion threshold. These nuclei (close to lead) reach their maximum deformation (dumbbell shape) at the saddle point. A large shell correction in the ground state affects strongly the level density in the neutron channel and leads to a high fission barrier (25–30 MeV). As a result, the fissility of preactinides is sensitive to both collective and shell effects. In addition, the compound nuclei formed from preactinide target nuclei are lighter and, therefore, much less fissile. For example, from Au to Ta ($\Delta Z = 6$) the electrofission cross section decreases by one order of magnitude between 100 and 200 MeV [13].

From the above, it would appear that the particular position of ^{232}Th, for which $Z^2/A \approx 35$, is very interesting because it lies in the transition region between nuclei with a single-humped fission barrier and nuclei with a double-humped fission barrier. Low energy monochromatic-photon data [9] show a strong increase of the fissility above the giant dipole resonance, from 20 to 40 MeV, followed by a slower increase in the quasideuteron region up to 110 MeV. No monochromatic-photon data are yet available above the pion threshold. From the bremsstrahlung data one can state only that, in the region 150–1000 MeV, the photofissility is lower than one and does not show clearly any energy behavior [3,4].

In this paper we report a measurement on ^{232}Th performed with tagged photons having energy between 250 and 1200 MeV; a simultaneous measurement on ^{238}U has been also performed and the data have been published elsewhere [5]. Because over a large part of the energy range investigated the total nuclear cross section is still not well known, in order to deduce the fissility of ^{232}Th we have assumed the fissility of ^{238}U to be unity, and the total nuclear cross section, deduced from ^{238}U data, has been scaled proportionally to the mass number A.

II. EXPERIMENT

The measurement was carried out at Frascati with the Jet Target tagged photon beam [14]. This beam was produced by tagging the bremsstrahlung from an internal target traversed by the electrons circulating in the ADONE storage ring. The radiator (Jet Target) was a molecular Argon beam crossing the ring vacuum pipe at supersonic speed [15], and was thin enough (about 10^{-10} radiation length) not to degrade the quality of the circulating beam so that several minutes of beam lifetime were assured [16]. The recoil electrons were momentum analyzed by the next ADONE dipole and were detected by two arrays of scintillation counters, 39 detectors in each, in coincidence. The scintillators defined 76 energy channels and were of different sizes in order to give a constant photon energy resolution at the maximum electron energy ($E_0 = 1500$ MeV) of 1% over the entire tagging range of $\Delta k = (0.4–0.8)E_0$. The photon energies from 250 to 1200 MeV were covered with different energy settings of the accelerator. In this measurement the tagger channels were summed four by four, since high energy resolution was not needed.

The experimental setup is shown in Fig. 2. Three magnets ($M1$, $M2$, and $M3$) swept charged particles away from the photon beam, which was defined in size by two collimators ($C1$ and $C2$) of diameter 6 and 12 mm, respectively. Two multiwire proportional chambers ($P1$ and $P2$) allowed the determination of the size of the photon beam to within 2 mm. Two thin plastic scintillators (NE 102A) were used as a relative photon beam monitor detecting in coincidence the Compton electrons and pairs produced by the photons in a thin (0.8 mm) gold converter positioned in front of the first scintillator. The stability of this simple device was found to be better than ±1%. A dense SF57 lead-glass detector was used as a photon spectrometer for the on-line measurement of the tagged

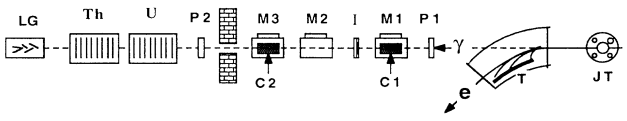

FIG. 2. Layout of the Jet Target tagged photon beam (not to scale): JT, Jet Target; T, tagging system; $P1$,$P2$, movable photon beam profile chambers; $M1$,$M2$,$M3$, sweeping magnets; $C1$,$C2$, collimators; I, relative intensity beam monitor; U and Th, parallel-plate avalanche detectors loaded with uranium and thorium; LG, lead-glass photon spectrometer.

photon flux incident on the target.

Two similar fission detectors, containing ^{238}U and ^{232}Th, were placed simultaneously in the photon beam, acting both as nuclear fissile targets and as fission-product detectors. The ^{232}Th fission detector was the parallel-plate avalanche detector (PPAD) described in Ref. [17], and has been used in a previous measurement at lower energy at Saclay [9]. It consisted of 58 aluminum plates (50 μm of thickness and 65 mm in diameter) coated on one side with a uniform deposition of $^{232}ThO_2$, having a total thickness of about 120 mg/cm^2. The plates were alternately connected to ground or to a potential of 430.0±0.1 V and the chamber was filled with isobutane maintained at a pressure of 7.60±0.01 mbar. Both voltage and pressure, whose changes would affect the detector gain and efficiency, were continuously controlled during data collecting. The contribution of the Al foils to the fission rate was measured and found to be negligible. This detector has the advantage of being quite insensitive to the electromagnetic background and of being nearly free from systematic errors associated with the geometry of the detector recording the fission fragments, since the angular distribution of the fragments has only a weak dependence on the energy of the primary photons.

A special calibration detector was installed inside the chamber together with the main PPAD detector to measure precisely its effective thickness, which is given by the product of the total thickness T, the efficiency ε, and the solid angle Ω for detection of the fission fragments. The calibration detector consisted of a single thin target of well-known thickness ($t_c = 196 \pm 4$ μg/cm^2) placed between two single PPADs; this setup could detect with efficiency ε_c equal to 1 the two fission fragments in coincidence and identify unambiguously the fission events. The solid angle Ω_c covered by the calibration detector was determined, with an uncertainty of 2%, by the measurement of the transverse distribution of the photon beam incident on the detector, by means of the wire profile chamber $P2$. The ratio of the counts of the calibration detector and the main detector with a full intensity bremsstrahlung beam is equal to the ratio $t_c\varepsilon_c\Omega_c/T\varepsilon\Omega$, from which we obtained the product $T\varepsilon\Omega$ of the main detector. As shown in Fig. 3, a nice plateau of this ratio was found for both fissile nuclei, changing the threshold for the calibration detectors, from about 50 mV to about 100 mV, and leaving unchanged the threshold for the main detectors. This result substantially corroborates the correctness of the assumption that $\varepsilon_c = 1$. This calibration method was slightly different than that used at Saclay [9], where an additional third background detector had to be used, because the transverse distribution of the photon beam on the PPAD could not be measured precisely, and thus the solid angle Ω_c.

The signals of every single PPAD of the main detector were amplified and discriminated to form a common OR signal. The coincidences $N_f(k)$ of the signals from a PPAD and the ith channel of the tagging system correspond to fissions of nuclei induced by photons of energy $k = E_0 - E_i$. The total number of photons $N_\gamma(k)$ in the ith energy bin incident on the target was determined by the coincidence of signals from the lead glass and the

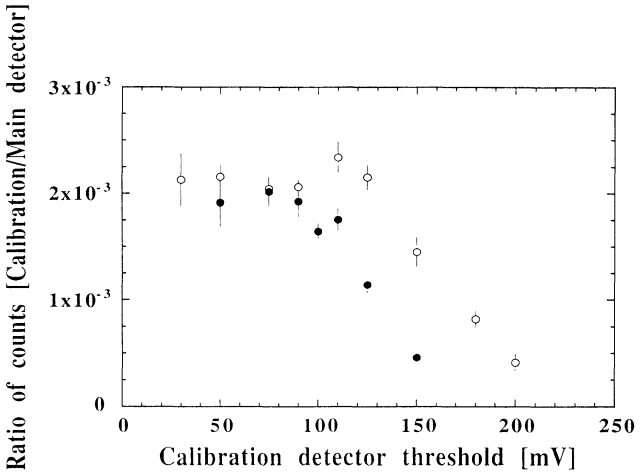

FIG. 3. Threshold curves of the ^{232}Th (closed circles) and ^{238}U (open circles) calibration detectors used to measure the effective thicknesses of the main ^{232}Th and ^{238}U target detectors.

counters of the ith channel of the tagging system. Random coincidences due to the electron beam time structure (a 1 ns wide pulse every 20 ns) and to the spontaneous α decay of the thorium target were measured on-line and then subtracted. The intensity of the beam was kept at a level of about 10^5 tagged photons/s.

Thus, the fission cross section $\sigma_f(k)$ was derived from the measured values of $N_f(k)$, $N_\gamma(k)$, and $T\varepsilon\Omega$, as follows:

$$\sigma_f(k) = \frac{N_f(k)}{N_\gamma(k)} \frac{A}{N_A T\varepsilon\Omega} ,$$

where N_A is the Avogadro number.

Data were obtained at five different electron beam energies (from 400 MeV to 1500 MeV) and the photon energy overlaps between different data sets indicated good control of systematic errors due to an imperfect knowledge of the photon beam flux and the tagging efficiency. The systematic errors have been estimated to be about 10% in the Δ region, decreasing to about 8% above 600 MeV: the larger systematic and statistical errors at low energies were due to the considerable increase of the collimator cuts on the lower energy photon beams, which reduced the tagging efficiency and increased the contribution of random coincidences.

III. RESULTS AND DISCUSSION

A. The photofission cross section

The photofission cross section $\sigma_f^{Th}(k)$ for ^{232}Th is shown in Fig. 4, where the experimental values have been divided by the mass number A and grouped in 30 MeV energy bins. Also shown are the data for ^{238}U [5] and the upper and lower limits of the "universal behavior" of the total photonuclear cross section in the Δ region [8].

The thorium data show that Δ excitation is the main absorption mechanism that results in fission in the region

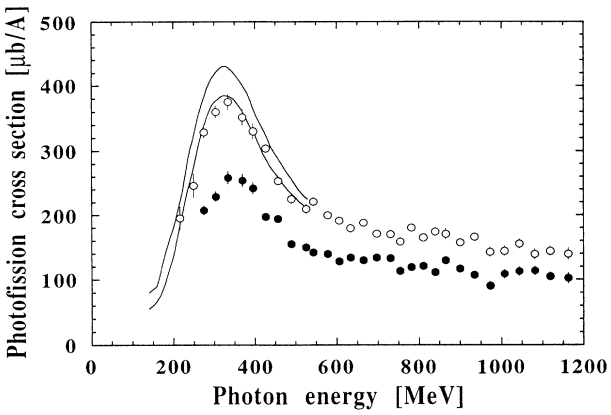

FIG. 4. The photofission cross section normalized to the mass number: present ^{232}Th data (closed circles) and ^{238}U data (open circles), Ref. [5]; the area between the two curves represents the universal behavior of the total nuclear cross section.

between 200 and 500 MeV. The maximum of the cross section is reached around 350 MeV, in good agreement with that found for the uranium data (and the universal curve for the total cross section). At energies higher than 500 MeV, both the ^{232}Th and ^{238}U data show no evidence of the excitation of the higher nucleonic resonances [mainly the $D_{13}(1520)$ and $F_{15}(1680)$] that are clearly seen in the total photoabsorption cross sections for the proton [18] and the deuteron [19]. This behavior might be explained by the broadening of the resonances due to mechanisms like Fermi motion or the propagation and interaction of the resonances in the nucleus. This effect was also observed in the measurements of the total photoabsorption cross section on beryllium and carbon recently carried out at Frascati [20,21].

B. The photofissility of ^{232}Th

To calculate the photofissility $W_f(k)$ of ^{232}Th from the measured photofission cross section $\sigma_f(k)$, we must know the total inelastic cross section $\sigma_T(k)$. Since this quantity is not available for ^{232}Th either from experimental data or from phenomenological model predictions, we proceeded as follows.

(1) We assumed the photofissility of ^{238}U to be equal to 1. This was shown, within the experimental errors, in very different regimes, like in the absorption of the photon by an n-p pair (quasideuteron region) [9] and in the resonance excitation through pion production (Δ resonance region) [5–7]. At higher energy, the comparison with the recent total cross section data for ^{9}Be and ^{12}C seems to confirm this statement up to 1200 MeV [20,21]; therefore we assumed that $\sigma_f^{\mathrm{U}}(k)=\sigma_T^{\mathrm{U}}(k)$ over the entire energy range of the present measurement.

(2) We assumed that, over the entire energy range of our investigation, the total photoabsorption cross section is proportional to the mass number A, as suggested by several experiments [5,8,20,21].

(3) Therefore, from the ratio $R(k)$ of the measured values for $\sigma_f^{\mathrm{Th}}(k)/A_{\mathrm{Th}}$ and for $\sigma_f^{\mathrm{U}}(k)/A_{\mathrm{U}}$ we obtained the thorium fissility:

$$W_f(k)=R(k)=\frac{\sigma_f^{\mathrm{Th}}(k)}{\sigma_f^{\mathrm{U}}(k)}\frac{A_{\mathrm{U}}}{A_{\mathrm{Th}}} .$$

These extracted values are shown in Fig. 5, where only the statistical errors are displayed. The contribution to the total error, due to the knowledge of the photon beam intensity and transverse distribution that are the main uncertainties of data in the Δ energy region, cancels in the ratio. Thus the systematic error for the fissility values was estimated to be 9% over the entire energy range. Also shown in the figure are the $R(k)$ values we have deduced, adopting the same procedure for the photofission data for ^{232}Th and ^{238}U measured by Leprêtre *et al.* [9] at lower energies. Moreover, we show the experimental value of $R(k)$ obtained from fission data for ^{232}Th and ^{238}U measured with 1 GeV protons [22]. The parent nuclei in this latter case were ^{233}Pa and ^{239}Np, but, as demonstrated in Ref. [23], the fission probability measured with different probes can be compared by selecting those initial energies for each probe which produce similar distributions of excitation energy E^*, angular momentum l, and nucleonic composition A_{CN} and Z_{CN}. Finally we calculated the mean value for $R(k)$ from all the nonmonochromatic photofission data for ^{232}Th and ^{238}U available in the literature above the pion threshold and up to 1 GeV [3,4]: we obtained the value of 0.64, in reasonable agreement with the mean value of 0.70 obtained from our data between 250 and 1000 MeV.

A simple visual inspection of Fig. 5 reveals, surprisingly, the following: (i) The photofissility values of ^{232}Th lie between 0.6 and 0.8, thus showing no saturation even at energies as high as 1200 MeV. (ii) The photofissility of ^{232}Th is a weak function of energy, increasing only about

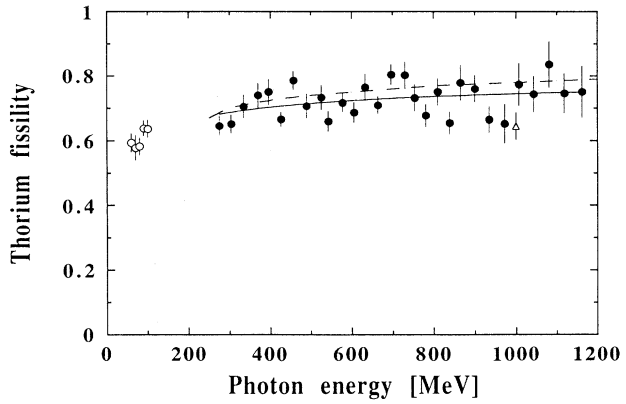

FIG. 5. Photofissility values for ^{232}Th obtained as described in the text (closed circles). Also shown are the values obtained with the same procedure from the data of Ref. [9] (open circles) and Ref. [25] (open triangle); the solid line is a fit of the form $\ln W_f(k)=A-Bk^{-1/2}$. The dashed line is the result of an INC calculation.

15% over an interval of 1 GeV. A simple function $\ln W_f(k) = A - Bk^{-1/2}$ fits well the energy behavior of our data. This energy parametrization, which reflects the approximate proportionality between the incident photon energy k and the mean excitation energy of the compound nucleus $\langle E^* \rangle$, was suggested in the past as a high energy limit [24], and was applied to various heavy nuclei [25,26]. (iii) An intranuclear cascade (INC) model prediction is also shown in Fig. 5: this model, which is exhaustively described in Ref. [27], is able to reproduce, at least qualitatively, the weak energy dependence of the experimental fissilities of ^{232}Th data, although it overestimates the absolute values.

C. Comparison with other nuclei

The comparison of the fissility of ^{232}Th with that of other nuclei could be made only up to the Δ region, due to the lack of higher energy data. In Fig. 6 we report the experimental fissility values W_f obtained at 300 MeV for some preactinides and actinides: specifically the ^{232}Th value from this experiment and the data for ^{197}Au, ^{209}Bi, ^{238}U, and ^{235}U, from previous photofission measurements. The total photoabsorption cross section is experimentally well known at this energy for all the nuclei and was taken equal to 400 μb/nucleon, corresponding to the mean value of the universal curves. As shown in Ref. [11], the compound nuclei, produced by 300 MeV photon impinging on nuclei from Au to U, have the same average values of mass and charge losses of $\langle \Delta A \rangle = 2$ and $\langle \Delta Z \rangle = 0.6$, respectively, and the distribution of these variables is similar. Due to the above considerations, the experimental fission cross sections, and hence the fissilities, are the results of an average over the ensemble of the compound nuclei produced in the reaction. In Fig. 6, the result of the intranuclear cascade calculation with the evaporation model is also shown for 300 MeV incident photons. The measured fissility shows a strong increase of about two orders of magnitude with the parameter Z^2_{CN}/A_{CN}, and

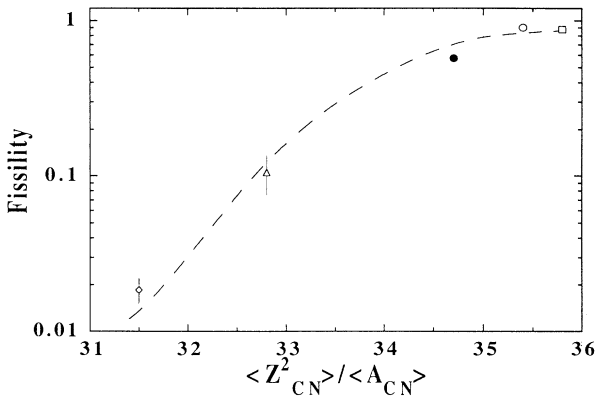

FIG. 6. Comparison of photofissility values for different nuclei measured with 300-MeV photons: ^{232}Th (closed circle), this work; ^{197}Au (diamond), Ref. [11]; ^{209}Bi (triangle), Ref. [12]; ^{238}U (open circle), Ref. [5]; ^{235}U (square), Ref. [7]. The dashed line is the result of an INC calculation.

this general behavior is fairly well reproduced by the INC simulation. However, it is worth noticing that in the actinide region ($Z^2_{CN}/A_{CN} \sim 35$), the clear increase of the experimental fissilty from ^{232}Th to ^{238}U is not reproduced by the INC prediction, and this might be an indication that not all of the physical mechanisms involved in the reaction are completely understood.

D. Nonsaturation of the photofissility of ^{232}Th: What could it mean?

The main experimental findings of this work, namely, the nonsaturation of the ^{232}Th photofissility and its weak dependence on the photon energy over the wide energy range from 250 to 1200 MeV, are both important. These findings were quite unexpected, taking into account that the photofissility of other actinides, like ^{235}U and ^{238}U, saturates at much lower energies (about 50 MeV). The analysis of data on nuclear fission provided by monochromatic intermediate energy photons, in the framework of the intranuclear-cascade evaporation model, allows us to investigate effects like the distribution in composition and excitation energy of compound nuclei, the thermal disappearance of shell effects, the dependence of fission barrier heights on the excitation energy, and the proper choice of the liquid drop model parameters [28]. Furthermore, this model does not reproduce in a precise way the photofissility of thorium measured relative to other actinides. At present there are no truly convincing explanations to account for this, so we can only introduce some reasonable phenomenological hypotheses. In a recent phenomenological study in the quasideuteron region, Delsanto *et al.* [29] explained the difference of photofissilities of ^{232}Th and ^{238}U by the change of active *n-p* pairs in processes which bring the excited compound system to fission. Precisely, this fact changes the nucleon scattering inside the nucleus and consequently its mean free path (or in other words the nuclear transparency). In our energy range, where the photopion reabsorption dominates, the same effect might be present, because pions are absorbed by *n-p* pairs. The key ingredient could be the relation between the quantities associated with the entrance channel (σ_T and k) and those describing the thermalized system (the compound nucleus formation probability σ_{CN} and E^*). In such a way the 30% difference in photofissility between otherwise similar nuclei like ^{232}Th and ^{238}U could be ascribed to some combination of the difference in σ_{CN} and the difference in the subsequent compound nucleus fission probability W_f.

Clearly, all of these issues require further theoretical studies. A phenomenological analysis of our results will appear soon [30].

IV. CONCLUSIONS

Here we summarize the main results and conclusions of our studies.

(a) We have measured the photofission cross section for ^{232}Th in the energy range 250–1200 MeV using a monochromatic tagged photon beam and multiplate PPADs.

(b) The photofission cross section clearly shows the ex-

citation of the Δ resonance, with a maximum at about 350 MeV. In the structure of the cross section there is no evidence of the higher nucleonic resonances, in agreement with the results obtained for ^{238}U and from total cross section measurements on ^{9}Be and ^{12}C.

(c) The ^{232}Th photofissility was calculated from the simultaneous measurement of the ^{238}U photofission cross section, assuming a fissility equal to 1 for the latter nucleus.

(d) In the energy range explored, the fissility values of ^{232}Th remain approximately between 0.6 and 0.8, showing a weak but clear increase with the energy, demonstrating that for this nucleus the saturation value still is not reached at 1200 MeV.

(e) A comparison with the prediction of an intranuclear-cascade evaporation Monte Carlo calculation was shown, but whereas the general behavior of fission processes was well reproduced, the agreement between the calculated and the measured fissility values is still unsatisfactory for actinide nuclei. The nonsaturation of the fissility of ^{232}Th also might be tentatively attributed to a possible smaller nuclear transparency.

The results presented in this paper strongly suggest the necessity of performing additional exclusive experiments with actinide and preactinide nuclei, over expanded energy regions and with different probes, measuring, if possible, the characteristics of both the fission fragments and the emitted particles.

ACKNOWLEDGMENTS

We would like to thank M. Albicocco, A. Macioce, A. Orlandi, W. Pesci, and A. Viticchiè for their continuous technical assistance and the ADONE staff for efficiency in running the machine. Three of us (A.D., A.S.I., and M.V.M.) express gratitude to the Istituto Nazionale di Fisica Nucleare for its warm hospitality, while another of us (J.D.T.A.-N.) thanks FAPESP (Brazil) for a travel grant.

[1] V. S. Barashenkov, F. G. Gereghi, A. S. Iljinov, and V. D. Toneev, Nucl. Phys. **A222**, 204 (1974).
[2] G. C. Baldwin and G. S. Klaiber, Phys. Rev. **71**, 3 (1947).
[3] B. Forkman and B. Schrøder, Phys. Scr. **5**, 105 (1972).
[4] *Photofission Above the Giant Resonance,* edited by B. G. Nedorezov and Y. Raniuk (Naukova Dumka, Kiev, 1989), pp. 68–73 (in Russian).
[5] N. Bianchi *et al.*, Phys. Lett. B **299**, 219 (1993).
[6] T. Frommhold, F. Steiper, W. Henkel, U. Kneissl, J. Ahrens, R. Beck, J. Peise, and M. Schmitz, Phys. Lett. B **295**, 28 (1992).
[7] J. Ahrens *et al.*, Phys. Lett. **146B**, 303 (1984).
[8] J. Ahrens, Nucl. Phys. **A446**, 229 (1985).
[9] A. Leprêtre *et al.*, Nucl. Phys. **A472**, 533 (1987).
[10] A. S. Iljinov, D. I. Ivanov, M. V. Mebel, V. G. Nedorzev, A. S. Sudov, and G. Ya. Kezerashvili, Nucl. Phys. **A539**, 263 (1992).
[11] V. Lucherini *et al.*, Phys. Rev. C **39**, 911 (1989).
[12] C. Guaraldo *et al.*, Phys. Rev. C **36**, 1027 (1987).
[13] J. D. T. Arruda-Neto, J. Phys. G (to be published).
[14] N. Bianchi *et al.*, Nucl. Instrum. Methods **A311**, 173 (1992).
[15] M. Taiuti *et al.*, Nucl. Instrum. Methods **A297**, 354 (1990).
[16] V. Muccifora *et al.*, Nucl. Instrum. Methods **A295**, 65 (1990).
[17] P. Garganne, Saclay Internal Report CEA-N-2492, 1986.
[18] T. A. Armstrong *et al.*, Phys. Rev. D **5**, 1640 (1972).
[19] T. A. Armstrong *et al.*, Nucl. Phys. **B41**, 445 (1972).
[20] M. Anghinolfi *et al.*, Phys. Rev. C **47**, 992 (1993).
[21] N. Bianchi *et al.*, Phys. Lett. B **309**, 5 (1993).
[22] L. A. Vaishnene, L. N. Andronenko, G. G. Kovshevny, A. A. Kotov, G. E. Solyakin, and W. Neubert, Z. Phys. A **302**, 143 (1981).
[23] A. S. Iljinov *et al.*, Phys. Rev. C **39**, 1420 (1989).
[24] J. R. Huizenga, R. Chaudry, and R. Vandenbosh, Phys. Rev. **126**, 210 (1962).
[25] L. G. Moretto, R. C. Gatti, S. G. Thompson, J. T. Routti, J. H. Heisenberg, L. M. Middleman, M. R. Yearian, and R. F. Hofstadter, Phys. Rev. **179**, 1176 (1969).
[26] J. D. T. Arruda-Neto, M. Sugawara, T. Tamae, O. Sasaki, H. Ogino, M. Miyase, and K. Abe, Phys. Rev. C **31**, 2321 (1985).
[27] V. S. Barashenkov, F. G. Gereghi, A. S. Iljinov, G. G. Jonssn, and V. D. Toneev, Nucl. Phys. **A231**, 462 (1974).
[28] A. S. Iljinov *et al.*, Nucl. Phys. **A543**, 570 (1992).
[29] P. P. Delsanto, A. Fubini, F. Murgia, and P. Quarati, Z. Phys. A **342**, 291 (1992).
[30] J. D. T. Arruda-Neto *et al.* (unpublished).